Amelie C. Jeanneau, Bertram Ostendorf, Tim Herrmann
Relative spatial differences in sediment transport in fire-affected agricultural landscapes: A field study
Aeolian Research, 2019; 39:13-22

Relative spatial differences in sediment transport in fire-affected agricultural landscapes: A field study

Amelie C. Jeanneau[a,*], Bertram Ostendorf[a], Tim Herrmann[b]

[a]School of Biological Sciences, The University of Adelaide, SA 5005 Australia

[b]Conservation and Sustainability, Department for Environment and Water, SA 5000 Australia

https://doi.org/10.1016/j.aeolia.2019.04.002

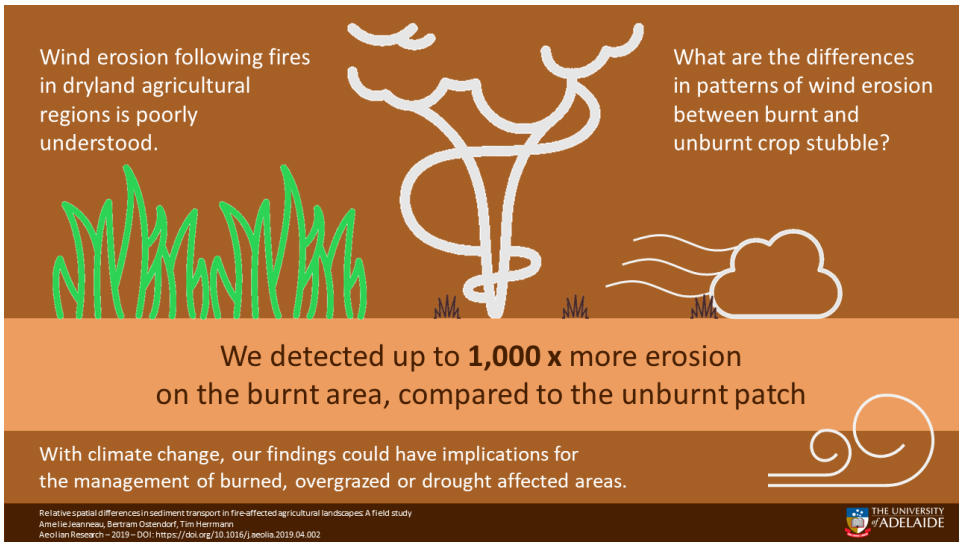

Abstract

Fires can considerably increase wind erosion risk in dryland agricultural regions. While wind erosion post-fire has been extensively studied in rangeland and grazing landscapes, limited work has considered post-fire erosion on annual plant communities and annual crops. Here we evaluated the relative spatial differences in patterns of sediment transport between burnt and unburnt crop stubble sites. Following a severe wildfire, we studied the spatio-temporal pattern of aeolian sediment transport with an array of Modified Wilson and Cooke (MWAC) dust samplers on adjacent burnt and unburnt wheat stubble. Sediment collection was conducted during nine weeks over an area of 3 hectares. Collection rates were converted to horizontal sediment flux to derive spatial distribution maps and perform statistical analysis. Compared to the unburnt plot, we observed that sediment transport was up to 1000 times higher within the burnt area. This could lead to damages to emerging annual crops sown after the fire if no management strategy was applied. There was only negligible sediment flux in areas with shallow and low-density stubble, which gradually increased with distance from the unburnt area. These results suggest that strips of remaining unburnt stubble could provide a potential benefit to adjacent burnt or bare plots. Patterns of sediment transport were consistent in all sampling periods and were observed at a spatial scale undetectable in wind tunnel studies, indicating that field observations could complement fine-scale experimental studies to assess environmental processes in real-life conditions.

Highlights

- Wind erosion following fires in dryland agriculture is little understood
- Sediment transport is high and spatially variable on burnt and bare patches
- Measuring field-scale sediment transport complements wind tunnel experimental studies
- Unburnt wheat stubble can reduce sediment transport on nearby burnt patches
- Findings will lead to improved management of dryland agriculture

Keywords

Aeolian transport; Fire; Sediment transport; Soil security; Spatial variability; Wind erosion

1. Introduction

Wind erosion strongly impacts agricultural productivity and public health. It generates on-site disturbances such as loss of topsoil leading to a decline in nutrients, organic matter and soil carbon, or damages to crops and infrastructure through sandblasting and burial (Bennell et al., 2007; Kontos et al., 2018; Panebianco et al., 2016). Consequences include the cost of nutrient replacement, purchase of new grain seeds and lost productivity. Wind erosion also generates off-site damages such as visibility limitation leading to road safety and transport issues, health impacts including asthma and other respiratory problems (Baddock et al., 2014; Li et al., 2018; Seinfeld and Pandis, 2012) as well as cleaning costs due to dust deposition and road maintenance. A substantial body of research have identified factors and parameters controlling wind erosion (Mayaud et al., 2017; Tatarko et al., 2013; Webb et al., 2016; Zobeck et al., 2003), but there is a paucity of studies relating soil erosion to consequences of extreme environmental disturbances like wildfires (Mayaud et al., 2017; Vermeire et al., 2005; Whicker et al., 2006).

Low rainfall agricultural regions in Mediterranean winter-rain climates are at high risk of soil loss due to a combination of low vegetation cover with potentially high wind events. Consequently, many studies have demonstrated that vegetation cover is the most effective way to control aeolian sediment transport (Chappell et al., 2019; McKenzie and Dixon, 2006; Shao, 2008; Vacek et al., 2018). Conservation agriculture is an increasingly common farming system in dryland agricultural regions as it aims to maintain vegetation cover for most of the year. In such areas, the erosion risk window generally occurs during autumn through to crop establishment or early winter. However, even with the best practices, catastrophic events and major types of disturbances such as wildfires can destroy the protective non-photosynthetic vegetation cover and increase erosion risk (Mayaud et al., 2017; Nordstrom and Hotta, 2004).

Fires are a dominant type of environmental disturbance, and they are unpredictable. They also remove protective vegetation cover of annual non-woody plants, increasing erosion risk in regions prone to wind erosion. Based on future climate forecast, in dryland agricultural regions, fires are expected to be more intense and more frequent, due to climate change, leading to an increase in erosion risk (Clarke et al., 2011; Gonçalves et al., 2011). In hot climates, even sparse vegetation can carry fires (Turner et al., 2011). Fires often occur during drier months, and if they occur early in the fire-danger season, they will leave soils bare for longer as summer rainfalls become more sporadic (CSIRO and Bureau of Meteorology, 2015; Williams et al., 2009).

Extensive research has studied wind erosion on agricultural croplands (Hagen, 1988; Retta et al., 1996; Tatarko et al., 2013; Zobeck et al., 2003), but there is limited evidence of the impact of fires in dryland

agriculture on wind erosion (Breshears et al., 2003; Ravi et al., 2012). Only a few studies directly compared wind erosion from burnt and unburnt plots simultaneously (Dukes et al., 2018; Merino-Martín et al., 2014; Miller et al., 2012; Wagenbrenner et al., 2013) and most of them only considered desert or grazing landscapes. Vegetation reduces wind velocity by applying a sheltering effect on exposed soil as clearly demonstrated in wind tunnel experiments and some field studies (Bilbro and Stout, 1999; Cornelis and Gabriels, 2005). However, there is a lack of information on the effect of unburnt vegetation patches on aeolian transport in cropped regions. Enhancing our predictive understanding of the link between erosion processes and catastrophic events such as wildfires is increasingly important in light of global climate change.

This study aims to assess the relative spatial differences in patterns of sediment transport between burnt and unburnt stubble patches after catastrophic wildfire events. Such information is challenging to obtain quantitatively because of their sizeable spatial extent and associated logistic difficulties to design controlled experiments, the rarity of wildfires in agricultural landscapes, and the emotional status of affected landholders after the fire. Here we report measurements taken after a severe wildfire that burnt 12,000 hectares of crops and pastures but left a small area of stubble unburnt which allowed for a paired sampling design.

2. Material and Methods

2.1. Site description

The study site is located near Keith in southern South Australia, Australia (Lat. 36°01'S, Long. 140°34'E, 73m elevation) (Figure 1). Mean annual precipitation for this district generally ranges between 350-450mm with predominant autumn-winter rainfall from May through to September. At the town of Keith, located 20km west of the site, mean annual maximum temperatures are of 22.3°C and mean annual minimum temperature of 9.1°C (Australian Bureau of Meteorology, http://www.bom.gov.au/climate/data/). Historically, most erosive and prevailing near-surface winds are from W to SW. Soils on the site are recorded as deep sands over clays, prone to wind erosion if unprotected.

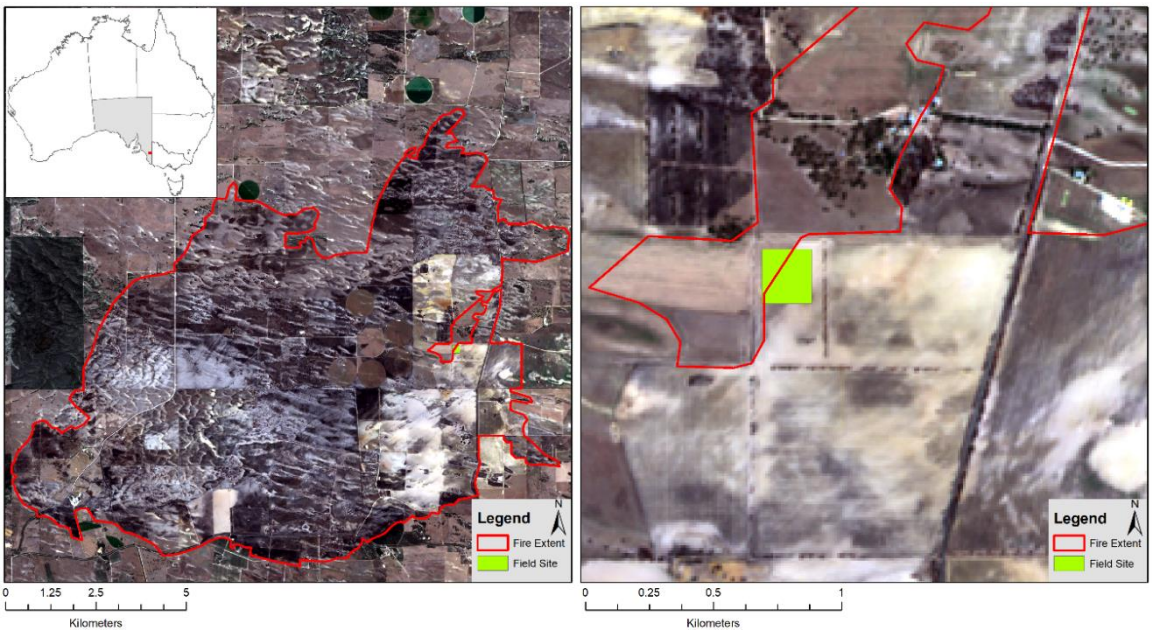

Figure 1: Location map and extent of the Sherwood fire, Sherwood, South Australia. The imagery was sourced from the European Space Agency (ESA) Copernicus – Sentinel 2 imagery, 03 February 2018. Within the fire boundary, darker colours represent charred vegetation; lighter cream colour represents exposed bare sands. Sand drifts can be observed predominantly in the south-eastern corner of fire extent.

The site was established on adjacent burnt and un-burnt wheat stubble following a severe fire that swept through the area between 6th and 7th January 2018. The study site was planted with a wheat crop with rows orientated North to South under no-till farm management. The field was harvested three weeks before the fire. To enhance water-holding capacity and improve the soil, this paddock was spread with clay five years ago. The land around the study site was also affected by the fire and spread with clay between the 9th and 23rd of March by the landholder as a recovery measure to increase surface roughness in an attempt to limit wind erosion.

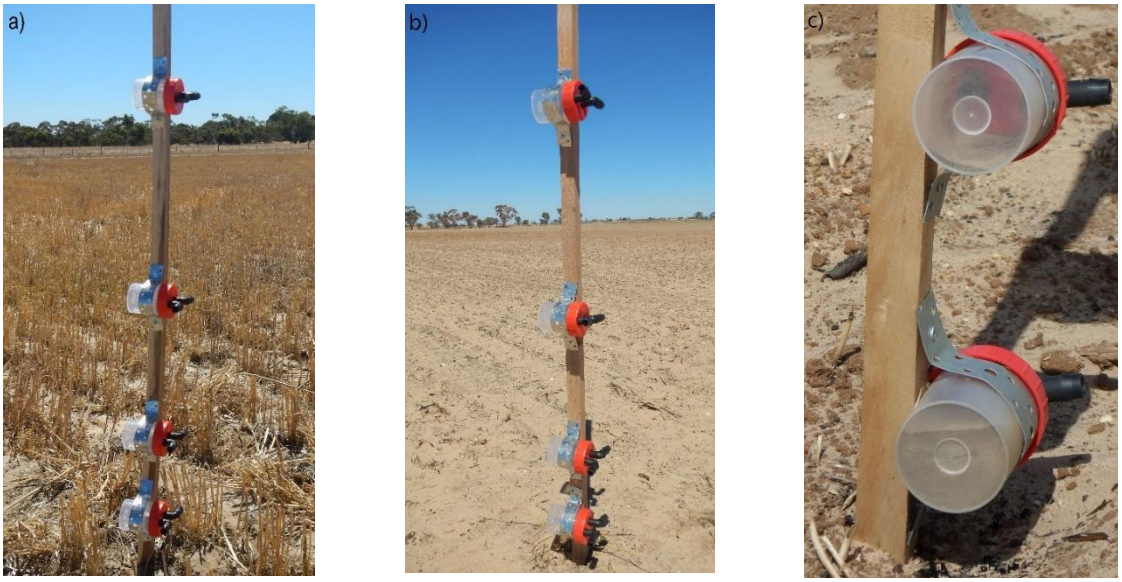

Figure 2: Dust samplers in the field, a) sediment sampler on unburnt wheat stubble, b) sediment sampler on the burnt bare ground, c) lower collecting cups filled with deposited sediment.

2.2. Monitoring design

Our monitoring design was adapted from the USDA (United States Department of Agriculture) wind erosion monitoring standardised methods (Webb et al., 2015). To monitor spatial variability in sediment transport influenced by fires, we established two 100m x 100m study plots within the same partly burned paddock. We set one site on unburnt wheat stubble (Figure 2a) and another on the adjacent bare ground (Figure 2b) with an exposed open fetch of about 300m by 150m extending to the south-west of the site. We will then refer to the treatments as unburnt and burnt. To improve the assessment of spatial patterns of sediment transport, we also installed sediment sampler every 40 m along a transect between the burnt and unburnt plots (Figure 3).

Horizontal sediment flux represents a measure of the wind-driven mass of sediments moving horizontally along the Earth surface at a particular height measured by a single sampler. Sediment transport was monitored with Modified Wilson and Cooke (MWAC) dust samplers (Wilson and Cooke, 1980). Preference was given to this type of equipment as they are efficient sediment traps, cost-effective and relatively easy to use and maintain. MWACs have a simple design: collection chambers are mounted on a rotating pole at four different sampling heights (0.1, 0.25, 0.5, 0.85m) with a wind vane that orients sampler inlets to face the wind. Due to manufacturing and time constraints, we decided to position the collector inlets to face the most dominant winds' direction (south-westerly winds). We acknowledge that this design has affected the efficiency of the MWAC collectors as they were not calibrated to collect airborne sediments in a single direction, however, this approach has been successfully applied by others to estimate the order of magnitude and spatial variability in local sediment transport (Farrell et al., 2012; Sherman et al., 2014; Van Jaarsveld, 2008).

In the standardised methods of Webb et al. (2015), the monitoring sites are divided into a 3x3 grid with three randomly located sediment samplers in each of the nine cells (total of 27 masts per site). The standard design was adopted in the burnt area, but due to the limited size of the unburnt patch, we could only establish a 2x3 grid with 18 masts in the unburnt section (Figure 3).

Due to emergency work required to limit soil erosion and land management constraints, monitoring commenced six weeks after the fire (26/Feb/2018), and samples were collected at three-week intervals over the next nine weeks (20/March, 12/April, 4/May). Half-hourly wind data was obtained from a local weather station in Keith (20km west of the site). Vegetation height and soil surface cover were estimated at site establishment on each plot along three 100m transects intersecting at 50m in the centre of the plot spaced by a 60° angle (Figure 3). Soil samples were taken following standard methods of Webb et al. (2015), and soil texture was defined by a hand texturing method (National Committee on Soil Terrain Committee, 2009).

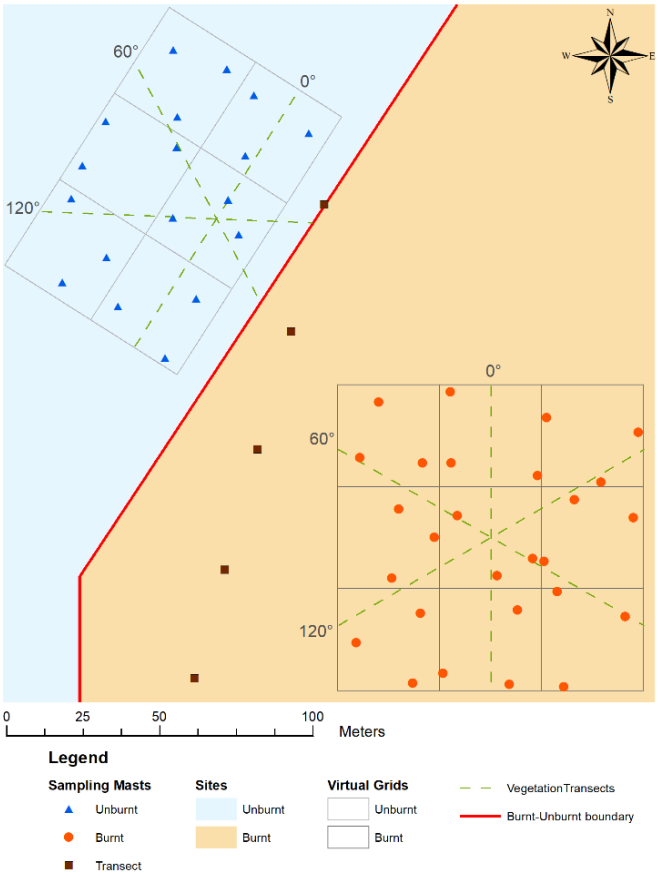

Figure 3: Experimental layout showing the spatial distribution of sampling masts and the position of the vegetation transects.

2.3. Sediment analysis

2.3.1. Horizontal sediment flux

After collection, sediments were dried in the lab and weighed on a high precision scale (0.0001g). We then converted the measurements to horizontal sediment mass flux by normalising the weight with tube inlet area (0.7854 cm^2) and the time of collection to obtain a time-averaged horizontal mass flux $q_{(z)}$ as

$$q_{(z)} = mass \times area^{-1} \times time^{-1} \quad (1)$$

where $mass$ is in g of sediments collected, $area$ is the size of the tube inlet area in m^2 and $time$ is the sampling interval in days. The units $q_{(z)}$ are expressed in grams per square metre opening per day.

The total observed horizontal sediment flux (Q_i) for a sampling mast i was estimated as the mean of time-averaged horizontal mass flux $q_{(z)i}$ over all collection heights using the following expression:

$$Q_i = \sum \left(q_{(10cm)i} + q_{(25cm)i} + q_{(50cm)i} + q_{(85cm)i}\right)/4 \quad (2)$$

where Q_i is expressed in grams per square metre opening per day.

This simple averaging approach has been used in similar settings (Belnap et al., 2009; Breshears et al., 2009; Duniway et al., 2015; Miller et al., 2012) but differs from standard methods using exponential decay functions to vertically integrate horizontal sediment flux estimates (Bergametti and Gillette, 2010; Gillette and Ono, 2008). However, sediment flux on the unburnt plot in our study area could not be described with an exponential decay function because the highest fluxes occurred at 50 cm and 85 cm height. Such pattern is likely due to the dust samplers being located in stable settings (wheat stubble) and primarily collected sediments generated far upwind or from the adjacent burnt area. Therefore, we chose to apply equation (2) to estimate the vertically averaged total horizontal sediment flux.

2.3.2. Spatial interpolation

In order to visualise how spatial patterns of sediment transport changed in time and with height, we generated maps of horizontal sediment mass flux (Q) for each collection period (Figure 5) and maps of time-averaged mass flux ($q_{(z)}$) for each sampling height over the total nine weeks (Figure 6). These maps were derived from sediment flux point data using Kriging (ArcGIS 10.5 Interpolation Toolbox with default parameters: spherical semi-variogram, variable search radius with 12 points, and output cell size of 0.9m). Kriging is a standard method of interpolation and was shown to be one of the most reliable two-dimensional spatial estimator (Chappell et al., 2003). We applied a mask to dim areas of high kriging uncertainty in the maps to aid visual interpretation of patterns. This mask was subjectively based on visual identification of areas with high kriging variance at the different sampling periods.

2.3.3. Statistical analysis

We used regression modelling to examine the relative influence and interactions of experimental parameters (horizontal and vertical dimensions, burnt/unburnt treatment, time) on horizontal sediment transport. Data preparation for the statistical analysis included the estimation of the shortest distance from each sampling mast to the burnt/unburnt boundary measured with the Proximity Toolbox (Near tool, ArcGIS 10.5). We employed linear mixed-effect models (*nlme* package, Pinheiro et al. (2018), R Development Core Team (2010)) for the regression analysis. In addition, we visualised the effect of distance to the burnt/unburnt boundary on sediment flux using LOESS regression.

Initial testing of regression modelling of horizontal sediment transport showed that residuals did not meet model assumptions of normality and constant variance. Normality of residuals was obtained through log-transformation of horizontal sediment flux. Variance changed within the study area, leading to a wide-tailed distribution of residuals that needed to be considered in the model structure.

Such a high variance was not surprising in an environment of high natural spatio-temporal variability of environmental factors (i.e. wind, soils, topography, canopy surface). The nlme mixed-effects models allow non-constant variance among sampling units. We initially used two models to explore if variance differed amongst grids, or whether those differences occurred among sampling locations at the within–grid scale. Examination of residuals and quantile-quantile plots indicated that the two linear mixed-effect models satisfied normality assumptions and hence the final model choice was based on the Akaike Information Criterion (AIC) (Akaike, 1973). This exercise revealed that finer scale sampling (point observations) better explained the variance in total horizontal sediment flux than grid level sampling (AIC_{mod1} = 596.5, AIC_{mod2} = 681.7). Similar method considerations were employed by Chappell et al. (2003) who observed that nested point sampling of airborne sediments outperformed grid and random sampling layouts.

Therefore, the final model structure used log-transformed horizontal sediment transport with the fixed effects treatment type (unburnt, burnt), direct distance to the burnt/unburnt boundary, collection period and height (with interactions between parameters) including all possible two-, three-, and four-way interactions. As random effects, we used the sampling grid location within the plots and the specific dust sampler's position within each grid of each plot.

3. Results

3.1. Meteorological conditions and surface cover

Wind direction was not constant in the region throughout the experiment. It predominately originated from the South and South-West in the first collection period with speeds up to 12.8m/s (46km/h), from the West-South-West and South-West in the second collection period with velocities up to 15m/s (54km/h) and from West to North with speeds up to 18.6m/s (67km/h) (Figure 4). Winds were the strongest in the final collection period. However, the weather remained mostly dry with less than 41mm of rain between 24/Feb/2018 and 04/May/2018, almost half of the precipitation has been recorded during a single event on 04/May/2018 (19mm). The average maximum daily temperature was recorded at 26.4°C for the length of our monitoring study.

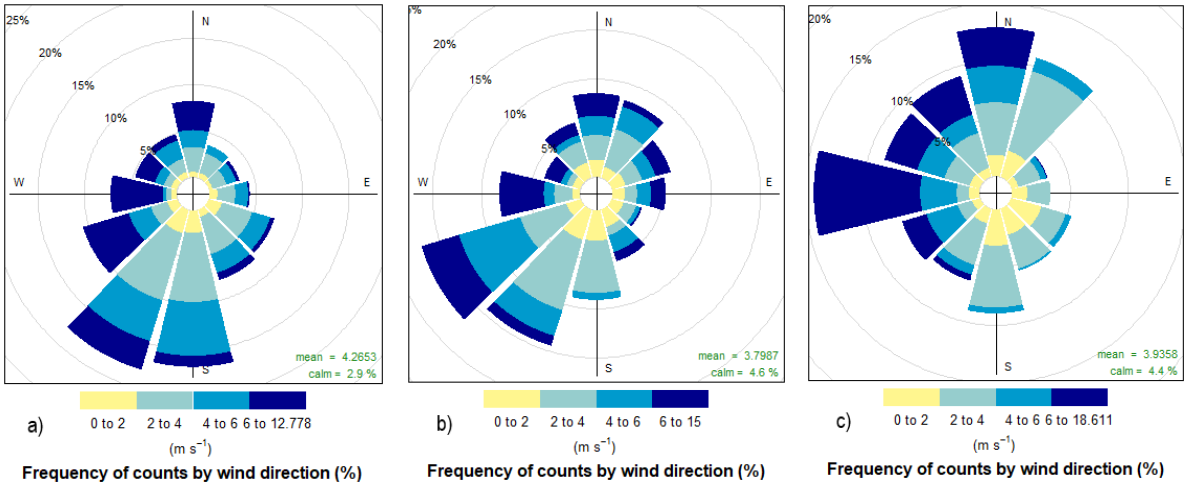

Figure 4: Wind roses representing wind speed and direction for the study area. a) collection weeks 1-3, b) collection weeks 4-6, c) collection weeks 7-9. Note the different frequency scale for collection week 7-9.

Wheat stubble on the unburnt patch had an average height of 20cm (±2cm) with a 20cm row spacing, and an average bare surface of 4.7% (±0.9%). Soil texture across the unburnt plot was sandy loam, and no soil crusting was observed at site establishment (Table 1). On the burnt plot, the fire consumed all of the vegetation (wheat stubble), only charred roots remained (1.3cm height ±0.7cm), and no regrowth was detected between February and May 2018. We recorded an average bare surface of 54% (±9.5%). Soil texture within the burnt plot was sandy loam, and soil crusting was observed on 47.6% (±2.9%) of the plot (Table 1).

Table 1: Summary of the soil surface conditions and vegetation states for the burnt and unburnt study plots, based on measurements collected

	Unburnt			**Burnt**		
	Transect 0°	*Transect 60°*	*Transect 120°*	*Transect 0°*	*Transect 60°*	*Transect 120°*
Soil texture	SL	SL	SL	SL	SL	SL
Vegetation state	Crop Stubble	Crop Stubble	Crop Stubble	Charred Roots, BS	Charred Roots, BS	Charred Roots, BS
Average vegetation height (cm)	20.2	19.7	20.2	1.4	1.4	1.2
Soil surface type	S, L, FG, GR	S, L, FG, GR	S, L, FG, GR	PC, S, L, FG, GR	PC, S, L, FG, GR	PC, S, L, FG, GR
Proportion of BS (%)	4	6	4	49	54	59
Proportion with PC surface type (%)	0	0	0	51	48	44
Proportion with FG surface type (%)	33	40	33	38	33	31
Proportion with GR surface type (%)	30	33	31	33	32	33

(**SL:** sandy loam, **BS:** bare soil, **S:** soil, **PC:** physical crust, **L:** litter, **FG:** fragments size 2-5mm, **GR:** 5mm < fragments size < 76mm)

3.2. Spatial distribution of sediment flux

When comparing the spatial distribution of total horizontal sediment flux (Q) between the three sampling dates, we can observe a recurring pattern common to all collection periods (Figure 5). Sediment transport was higher in the south-eastern corner of the burnt plot, which was the furthest away from the unburnt stubble boundary. There was also more spatial variability in horizontal sediment flux within the burnt plot compared to the unburnt patch. Total horizontal sediment flux in the last collection period (weeks 7-9) has almost decreased by half. Even if winds were the strongest during this collection period, the low sediment transport recorded could be explained by the fact that dust samplers were facing South-West and North-East directions while winds mostly originated from West to Northerly angles. Additionally, the last collection period recorded wetter conditions than the other two (37mm as opposed to 1.5mm) which could have also impacted the quantity of sediment collected.

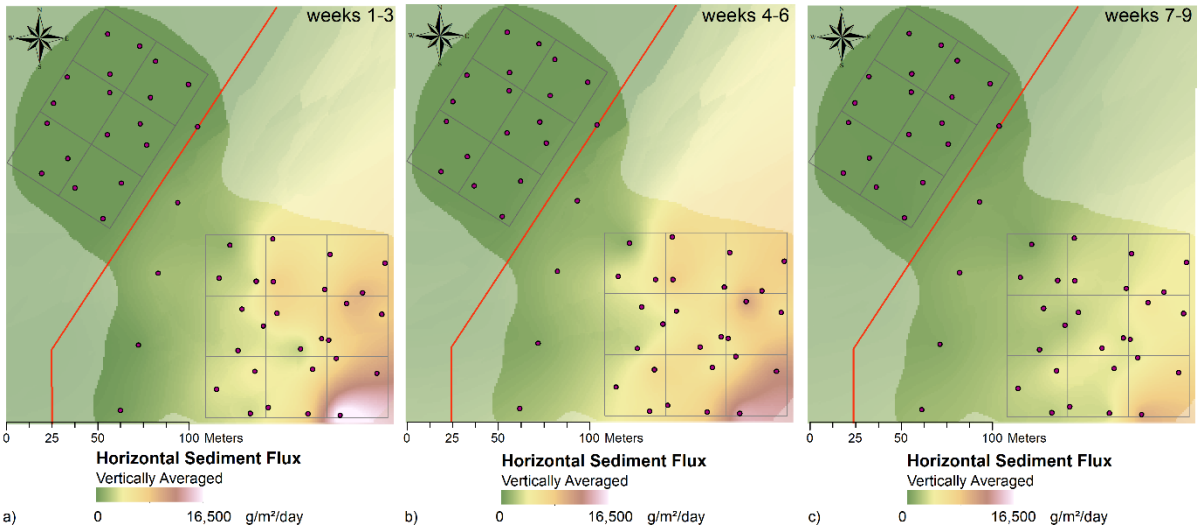

Figure 5: Vertically averaged horizontal sediment flux spatial distribution maps. a) collection weeks 1-3, b) collection weeks 4-6, c) collection weeks 7-9. The dots represent the MWAC dust sampler, and the two virtual sampling grids are outlined in grey.

Height-resolved time-averaged horizontal sediment flux: $q_{(z)}$ (mean of all collection periods) indicates similar spatial distribution patterns for each sampling height (Figure 6). These maps illustrate that total horizontal sediment flux increased with the direct distance from the unburnt stubble into the exposed part and reached its highest value in the south-eastern corner of the burnt plot.

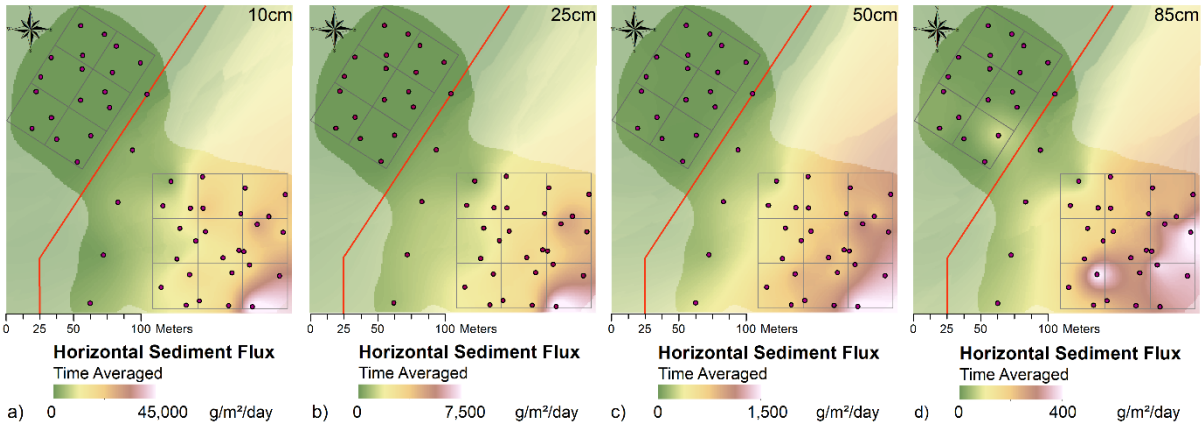

Figure 6: Mean horizontal sediment flux for the study at a) 10cm, b) 25cm, c) 50cm and d) 85cm sampling height. The purple dots represent the position of each MWAC dust samplers. Note large differences in sediment flux with height as indicated by different colour scales, ranging from 0 to maximum value.

Sediment movement was low in the unburnt plot and within the first 25-50m from the unburnt stubble, but steadily intensified with direct distance from the burnt-unburnt boundary (Figure 6, Figure 7).

As previously reported in other wind erosion studies, we observed that sediment transport rapidly decreased with height. Additionally, we can notice from the legend scale of Figure 6 and Figure 7 that there is a very large difference in horizontal sediment flux between the collection height of 10cm and the other sampling heights.

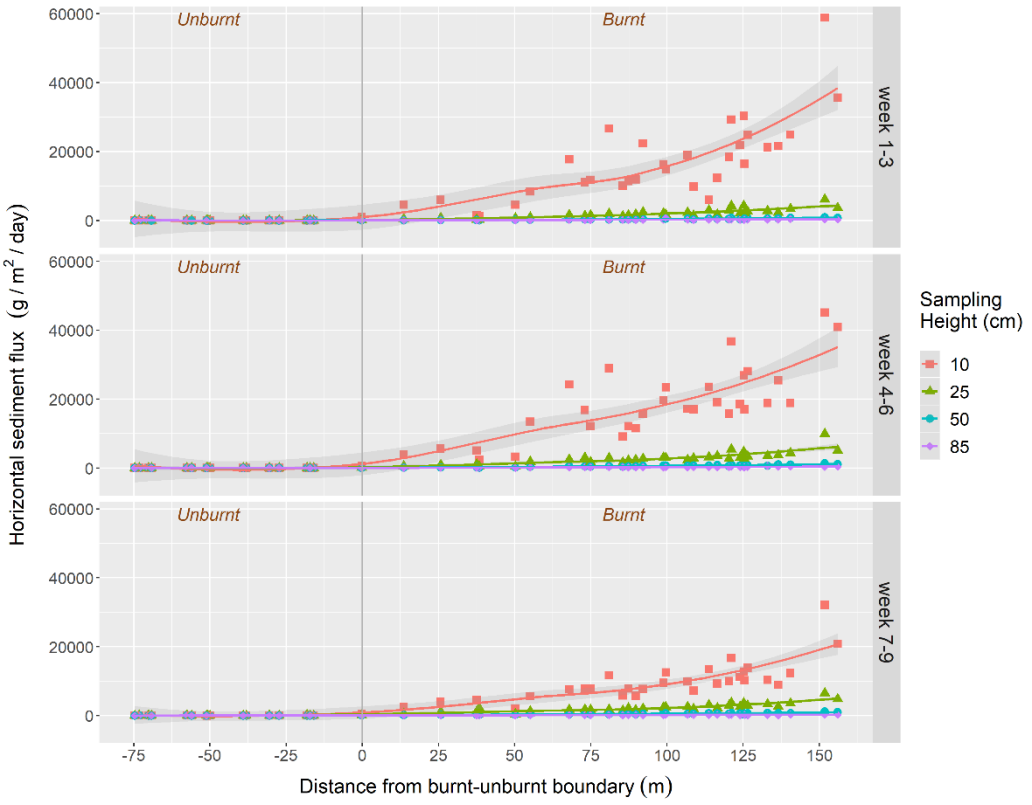

Figure 7: Observed horizontal sediment flux distribution with sampling distance from the burnt-unburnt boundary. 95% confidence interval of the LOESS regressions are shown as shaded grey bands.

3.3. Factors influencing horizontal sediment flux

The mixed-effects model allowed detailed examination of main effects and interactions between all the experimental factors (*Treatment:* unburnt/burnt; direct *Distance* to the burnt-unburnt boundary; sampling *Height*; *Time:* collection period, Table 2). Our results indicate that all four variables had a significant impact on total horizontal sediment flux ($p < 0.001$). More specifically, the interaction between treatment type and other individual factors had a significant effect on sediment transport ($p \leq 0.0001$). This information reflects that the magnitude of sediment transport on the burnt plot compared to the unburnt part of the site varies independently from the collection period or collection height (Figure 5 and Figure 6). The strongest interaction is that of *Treatment x Height*. In the burnt area, sediment flux follows an exponential decline, whereas, in the stubble, sediment is lowest in the bottom collection containers. The strong significance underpins this observation. We also observed that the interaction between sampling height and collection period had a significant impact of on total horizontal sediment flux ($p < 0.001$). This finding supports visual patterns in Figure 7 where horizontal sediment flux is lower during the third collection period (week 7-9) for all sampling heights, particularly for the 10cm sampling height. This can be expected due to changes in wind speed and direction throughout the experiment. The only significant three-way interaction identified in our model was between treatment type, collection height and time ($p < 0.001$). This indicates that the strongest two-way interaction (*Treatment x Height*) also differs in time. This observation also reflects the stochastic nature of wind causing a significant spatial variability in sediment flux with height.

Table 2: Estimated effect of experimental variables on sediment transport, obtained from linear mixed-modelling and Anova Wald Chi-square test, type II.

Source	χ^2	d.f	p-value	Significance
Treatment (unburnt/burnt)	248.0444	1	< 0.0001	***
Dist (distance to burnt-unburnt boundary)	43.7216	1	< 0.0001	***
Height (dust sampling height)	16966.8615	3	< 0.0001	***
Time (collection period)	342.7610	2	< 0.0001	***
Treatment*Dist	14.7704	1	0.0001	***
Treatment*Height	895.4564	3	< 0.0001	***
Treatment*Time	17.7556	2	0.0001	***
Dist*Height	8.2086	3	0.0419	ns
Dist*Time	9.3862	2	0.0092	**
Height*Time	83.3022	6	< 0.0001	***
Treatment*Dist*Height	2.5118	3	0.4731	ns
Treatment*Dist*Time	4.7756	2	0.0918	ns
Treatment*Height*Time	24.8422	6	0.0004	***
Dist*Height*Time	6.2830	6	0.3922	ns
Treatment*Dist*Height*Time	3.9544	6	0.6829	ns

(d.f = degree of freedom, ns = not significant, ** = p<0.01, *** = p<0.001)

This significance was investigated further by a comparison of the estimated marginal means of sediment flux grouped by treatment, height, and time (Figure 8). Mean horizontal sediment flux was low for all collection periods and all heights on the unburnt plot (~16 g/m^2/d) (Figure 8). Conversely, sediment transport was consistently higher on the burnt part of the site (100 - 8,000 g/m^2/d). Flux on the burnt plot was about 300 times larger than on the unburnt part of the site and within a similar order of magnitude of results published by Miller et al. (2012). Within the first four months of their post-fire study, the authors reported mean horizontal sediment fluxes of ~24 g/m^2/d on unburnt sites and ~2,400 g/m^2/d on burnt monitoring sites.

Mean collection rates from our experiment ranged from 0.001 g/d on the unburnt plot to 0.39 g/d on the burnt part of the site. These values are comparable to findings from Whicker et al. (2002) where they recorded median collection rates ranging from 0.1 g/d on unburnt sites to 0.3 g/d on burnt sites.

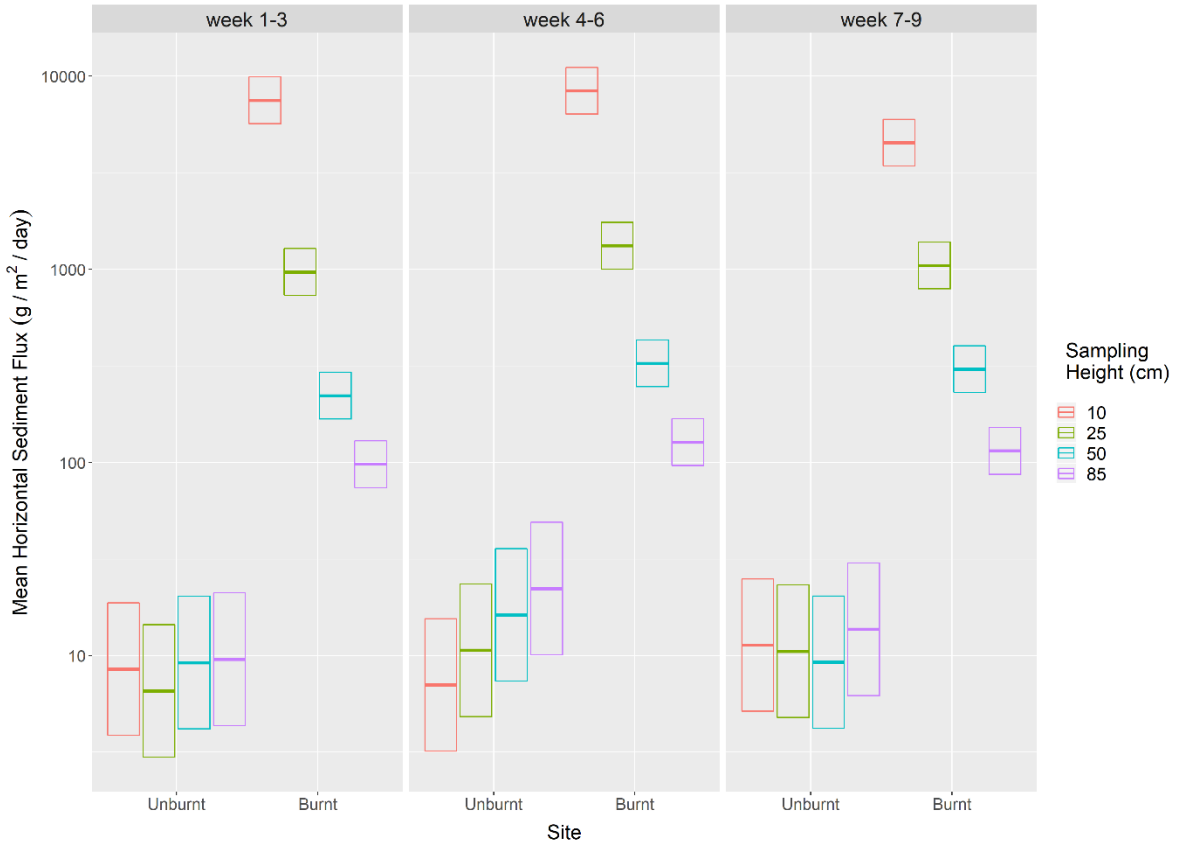

Figure 8: Mean horizontal sediment flux derived from modelled estimated marginal means for the three collection periods on burnt and unburnt plots. Estimates are based on log-scale predictions from the model.

The mean horizontal sediment flux on the burnt plot rapidly decreased with sampling height for all three collection periods (Figure 8), which is consistent in space and time (Figure 6 and Figure 7). This observation also supports results reported in other wind erosion studies (Bergametti and Gillette, 2010; Gillette and Ono, 2008). Additionally, the difference in sediment transport between the burnt and unburnt plots was highly significant, even at the upper sampling point. We detected a 10-fold

difference at 85cm, a 100-fold difference at 50cm and a 1,000-fold difference at 10cm for all collection periods

4. Discussion

This work has detected a significant difference in spatial distribution patterns between burnt and unburnt stubble plots after a severe wildfire event. Under the experimental conditions and throughout the three collection periods, we consistently observed a large aeolian sediment transport on the burnt part of the site and minimal sediment flux within the unburnt plot.

Our experimental design was limited by the nature and the pattern of the wildfire, as well as the land management actions required for remediation and erosion mitigation. Finding collaboration partners proved to be challenging given the emotional status of affected landholders. Furthermore, to increase the number of sampling locations, we decided to compromise on sampling directionality. In order to assess spatial patterns of sediment transport in burnt and unburnt areas, we used a simple unidirectional design and focussed on the prevailing wind direction in the region during that time of the year. The performance of our MWAC sediment samplers was thus limited by the fact that they could not face the wind during each wind event causing a potential underestimation of our sediment flux estimates. Based on the literature, the efficiency of our samplers might only be about 20 to 50% (Zobeck, 2002). While our approach reduced comparability with other studies, this proved to be successful for our study objectives, as we repeatedly collected a large amount of sediments on the burnt plot (Figure 2c, Figure 5), and consistently observed significant spatial distribution patterns of sediment transport regardless of wind speed and wind direction (Figure 5, Figure 6).

There were substantial differences in sediment transport in the height profile between the burnt and unburnt plots (section 0). In the burnt area, our data show a 10-fold difference at 85cm, a 100-fold difference at 50cm and a 1,000-fold difference at 10cm for all collection period, over all wind directions compared to the unburnt patch. These large amounts of sediment observed on the burnt side consistently exhibited exponential decline with height, whereas, over the stubble, height response was flat or increased with height. This is underpinned by the significant three-way interaction of treatment, height, and time. In fact, during the second collection period (weeks 4-6), most sediments were collected in the highest samplers. This indicates a potential influence of stubble on sediment flux as sediments captured on the unburnt part of the site may have originated from the burnt site. The observed inversion of exponential decline detected on the unburnt plot hence supports the supposition that stubble prevented aeolian sediments from forming. Differences of wind speed

and direction and sediment load from the burnt site moving into the unburnt patch may also explain heteroscedasticity between observation points and the need to use mixed models.

The consistent increase of sediment flux with distance from the burnt/unburnt boundary further supports that sediment transport was generated in the burnt patch, while saltation was prevented in the stubble area. Given that the field length was about 300m long by 150m wide, we may not have reached maximum transport carrying capacity. According to Zobeck et al. (2003), a field length of approximately 300m is needed in open agricultural fields with fine sandy loam soils to approach saltation transport capacity and assess total soil loss. However, in their study, horizontal sediment flux continued to increase at distances greater than 350m. This implies that our experimental design may not have sampled the total soil loss from the burnt site, but mainly captured local sediment redistribution instead.

Sediments generated in the burned area may have implications for land management. Sandblasting after a wildfire event may damage emerging seedlings from subsequent annual crops. There is anecdotal evidence from farmers who observed growing tillers to be sheared off in similar settings. Therefore, remediation and crop growth efficiency could be significantly reduced if wind erosion events occur before crop establishment.

We observed patterns of sediments transport within our burnt plot at a scale that is unachievable in controlled experiments. This indicates that field observations, albeit under less controlled conditions, can complement fine-scale experimental studies using wind tunnels to assess environmental processes. Although aeolian transport was very high on the burnt part of the site, it might have approached even higher values outside of our sampling range when maximum transport carrying capacity was reached.

5. Conclusion

Wind erosion is a key factor causing land degradation in dryland agricultural regions around the world. In such regions, soil cover is a critical erosion control factor and conservation agriculture is contributing to erosion mitigation. However, unpredictable extreme environmental disturbances such as wildfires can remove protective vegetation cover and consequently increase soil erosion risk.

In this study, an array of aeolian sediment samplers was established on adjacent burnt and unburnt sections of a paddock to assess relative spatial differences in patterns of sediment transport. This spatial array could be rapidly installed after a severe wildfire and proved to capture the spatial variability of aeolian sediment transport within the sites, regardless of wind velocity and direction.

Our findings indicate that sediment transport was very high and variable within the burnt and bare plots. These results could imply that annual crops sown after the fire may be at risk of sandblasting if one or several erosion events occurred before crop establishment, leading to serious implications for land management and productivity. However, we estimated that sediment transport was greatly reduced within the unburnt stubble plot and its vicinity into the burnt area. Based on our results, we can suggest that strips of remaining unburnt stubble could provide a beneficial effect on adjacent burnt or bare plots. Therefore, any management strategy that adds or maintains roughness elements, such as conservation farming and no-tillage, could reduce the risk of soil loss in degraded environments. Some of these may include strip cropping or soil treatments (e.g. clay spreading, soil mixing), particularly on light sandy soils. Nonetheless, such options may not always be practical or economically viable in agricultural production systems. There will thus be a need to find a balance between soil conservation, agricultural productivity and practicality when it comes to wind erosion management.

Our study also supports the argument that field observations can complement fine-scale experimental studies to assess environmental processes in real-life conditions. Indeed, we measured a large sediment transport on the burnt part of the site, but the scale at which we observed these distribution patterns would not have been detected in wind tunnel experiments.

While our study focused on fire as a cause of soil exposure, extended drought and overgrazing may also produce large patches of bare soils. Here, small areas of remnant vegetation may substantially reduce soil losses.

Acknowledgements

We wish to thank Stephen Jaeschke and his family for their involvement in the project and for supporting our monitoring study on their land despite being personally impacted by the fire. We also want to express our gratitude to Claire Dennerley for her assistance in the field, Steven Delean for his advice on statistical analysis, and the anonymous reviewers, whose suggestions significantly improved the quality of the manuscript. This research was supported by an International Postgraduate Scholarship Award.

Declaration of interest

We wish to confirm that there are no known conflicts of interest associated with this publication and there has been no significant financial support for this work that could have influenced its outcome.

References

Akaike, H., 1973. Information theory and an extension of the maximum likelihood principle, in: Petrov, B.N., Csaki, F. (Eds.). Akadémiai Kiadó, Budapest, Hungary, pp. 267-281, doi: https://doi.org/10.1007/978-1-4612-1694-0_15.

Baddock, M.C., Strong, C.L., Leys, J.F., Heidenreich, S.K., Tews, E.K., McTainsh, G.H., 2014. A visibility and total suspended dust relationship. Atmospheric Environment 89, 329-336, doi: https://doi.org/10.1016/j.atmosenv.2014.02.038.

Belnap, J., Reynolds, R.L., Reheis, M.C., Phillips, S.L., Urban, F.E., Goldstein, H.L., 2009. Sediment losses and gains across a gradient of livestock grazing and plant invasion in a cool, semi-arid grassland, Colorado Plateau, USA. Aeolian Research 1, 27-43, doi: https://doi.org/10.1016/j.aeolia.2009.03.001.

Bennell, M.R., Leys, J.F., Cleugh, H.A., 2007. Sandblasting damage of narrow-leaf lupin (Lupinus angustifolius L.): a field wind tunnel simulation. Soil Research 45, 119-128, doi: https://doi.org/10.1071/SR06066.

Bergametti, G., Gillette, D., 2010. Aeolian sediment fluxes measured over various plant/soil complexes in the Chihuahuan desert. Journal of Geophysical Research: Earth Surface 115, doi: https://doi.org/10.1029/2009JF001543.

Bilbro, J.D., Stout, J.E., 1999. Wind velocity patterns as modified by plastic pipe windbarriers. Journal of Soil and Water Conservation 54, 551-556,

Breshears, D.D., Whicker, J.J., Johansen, M.P., Pinder, J.E., 2003. Wind and water erosion and transport in semi-arid shrubland, grassland and forest ecosystems: Quantifying dominance of horizontal wind-driven transport. Earth Surface Processes and Landforms 28, 1189-1209, doi: https://doi.org/10.1002/esp.1034.

Breshears, D.D., Whicker, J.J., Zou, C.B., Field, J.P., Allen, C.D., 2009. A conceptual framework for dryland aeolian sediment transport along the grassland–forest continuum: effects of woody plant canopy cover and disturbance. Geomorphology 105, 28-38, doi: https://doi.org/10.1016/j.geomorph.2007.12.018.

Chappell, A., McTainsh, G., Leys, J., Strong, C., 2003. Simulations to optimize sampling of aeolian sediment transport in space and time for mapping. Earth Surface Processes and Landforms 28, 1223-1241, doi: doi:10.1002/esp.1036.

Chappell, A., Webb, N.P., Leys, J.F., Waters, C.M., Orgill, S., Eyres, M.J., 2019. Minimising soil organic carbon erosion by wind is critical for land degradation neutrality. Environmental Science & Policy 93, 43-52, doi: https://doi.org/10.1016/j.envsci.2018.12.020.

Clarke, H.G., Smith, P.L., Pitman, A.J., 2011. Regional signatures of future fire weather over eastern Australia from global climate models. International Journal of Wildland Fire 20, 550-562, doi: https://doi.org/10.1071/WF10070.

Cornelis, W.M., Gabriels, D., 2005. Optimal windbreak design for wind-erosion control. Journal of Arid Environments 61, 315-332, doi: https://doi.org/10.1016/j.jaridenv.2004.10.005.

CSIRO, Bureau of Meteorology, 2015. Climate Change in Australia Information for Australia's Natural Resource Management Regions: Technical Report. CSIRO and Bureau of Meteorology, Australia, https://www.climatechangeinaustralia.gov.au/media/ccia/2.1.6/cms_page_media/168/CCIA_2015_NRM_TechnicalReport_WEB.pdf

Dukes, D., Gonzales, H.B., Ravi, S., Grandstaff, D.E., Van Pelt, R.S., Li, J., Wang, G., Sankey, J.B., 2018. Quantifying Postfire Aeolian Sediment Transport Using Rare Earth Element Tracers. Journal of Geophysical Research: Biogeosciences 123, 288-299, doi: https://doi.org/10.1002/2017JG004284.

Duniway, M.C., Palmquist, E., Miller, M.E., 2015. Evaluating rehabilitation efforts following the Milford Flat Fire: successes, failures, and controlling factors. Ecosphere 6, art80, doi: https://doi.org/10.1890/ES14-00318.1.

Farrell, E.J., Sherman, D.J., Ellis, J.T., Li, B., 2012. Vertical distribution of grain size for wind blown sand. Aeolian Research 7, 51-61, doi: https://doi.org/10.1016/j.aeolia.2012.03.003.

Gillette, D.A., Ono, D., 2008. Expressing sand supply limitation using a modified Owen saltation equation. Earth Surface Processes and Landforms 33, 1806-1813, doi: https://doi.org/10.1002/esp.1736.
Gonçalves, A.B., Vieira, A., Leite, F.F., Martins, J., Silva, D., Soares, V., 2011. ADAPTACLIMA: adaptation to the effects from climate change in the AVE, 3rd International Meeting of Fire Effects on Soil Properties. Nigp-Univ. Minho e Cegot, pp. 175-180, http://hdl.handle.net/1822/19983
Hagen, L., 1988. New wind erosion model developments in the USDA, 1988 Wind Erosion Conference Proceedings. Texas Tech. University, Lubbock, pp. 11-13,
Kontos, S., Liora, N., Giannaros, C., Kakosimos, K., Poupkou, A., Melas, D., 2018. Modeling natural dust emissions in the central Middle East: Parameterizations and sensitivity. Atmospheric Environment 190, 294-307, doi: https://doi.org/10.1016/j.atmosenv.2018.07.033.
Li, J., Kandakji, T., Lee, J.A., Tatarko, J., Blackwell, J., Gill, T.E., Collins, J.D., 2018. Blowing dust and highway safety in the southwestern United States: Characteristics of dust emission "hotspots" and management implications. Science of The Total Environment 621, 1023-1032, doi: https://doi.org/10.1016/j.scitotenv.2017.10.124.
Mayaud, J.R., Bailey, R.M., Wiggs, G.F.S., 2017. A coupled vegetation/sediment transport model for dryland environments. Journal of Geophysical Research-Earth Surface 122, 875-900, doi: https://doi.org/10.1002/2016jf004096.
McKenzie, N., Dixon, J., 2006. Monitoring soil condition across Australia. Recommendations from expert panels. Prepared for the National Committee on Soil and Terrain for the National Land and Water Resources Audit, http://lwa.gov.au/products/pn21340
Merino-Martín, L., Field, J.P., Villegas, J.C., Whicker, J.J., Breshears, D.D., Law, D.J., Urgeghe, A.M., 2014. Aeolian sediment and dust fluxes during predominant "background" wind conditions for unburned and burned semiarid grassland: Interplay between particle size and temporal scale. Aeolian Research 14, 97-103, doi: https://doi.org/10.1016/j.aeolia.2014.02.004.
Miller, M.E., Bowker, M.A., Reynolds, R.L., Goldstein, H.L., 2012. Post-fire land treatments and wind erosion – Lessons from the Milford Flat Fire, UT, USA. Aeolian Research 7, 29-44, doi: https://doi.org/10.1016/j.aeolia.2012.04.001.
National Committee on Soil Terrain Committee, 2009. Australian Soil and Land Survey Field Handbook. CSIRO PUBLISHING, Victoria,
Nordstrom, K.F., Hotta, S., 2004. Wind erosion from cropland solutions in the USA: a review of problems, and prospects. Geoderma 121, 157-167, doi: https://doi.org/10.1016/j.geoderma.2003.11.012z.
Panebianco, J.E., Mendez, M.J., Buschiazzo, D.E., 2016. PM10 Emission, Sandblasting Efficiency and Vertical Entrainment During Successive Wind-Erosion Events: A Wind-Tunnel Approach. Boundary-Layer Meteorology 161, 335-353, doi: https://doi.org/10.1007/s10546-016-0172-7.
Pinheiro, J., Bates, D., DebRoy, S., Sarkar, D., Team, R.D.C., 2018. nlme: Linear and Nonlinear Mixed Effects Models, R package version 3.1-137 ed, https://CRAN.R-project.org/package=nlme
R Development Core Team, 2010. R: A Language and Environment for Statistical Computing. R Foundation for Statistical Computing, Vienna, Austria, http://www.R-project.org
Ravi, S., Baddock, M.C., Zobeck, T.M., Hartman, J., 2012. Field evidence for differences in post-fire aeolian transport related to vegetation type in semi-arid grasslands. Aeolian Research 7, 3-10, doi: http://dx.doi.org/10.1016/j.aeolia.2011.12.002.
Retta, A., Armbrust, D.V., Hagen, L.J., 1996. Partitioning of biomass in the crop submodel of WEPS (wind erosion prediction system). Transactions of the Asae 39, 145-151, <Go to ISI>://WOS:A1996TX42700020
Seinfeld, J.H., Pandis, S.N., 2012. Atmospheric chemistry and physics: from air pollution to climate change. John Wiley & Sons,
Shao, Y., 2008. Physics and modelling of wind erosion. Springer Science & Business Media,
Sherman, D.J., Swann, C., Barron, J.D., 2014. A high-efficiency, low-cost aeolian sand trap. Aeolian Research 13, 31-34, doi: https://doi.org/10.1016/j.aeolia.2014.02.006.

Tatarko, J., Sporcic, M.A., Skidmore, E.L., 2013. A history of wind erosion prediction models in the United States Department of Agriculture prior to the Wind Erosion Prediction System. Aeolian Research 10, 3-8, doi: https://doi.org/10.1016/j.aeolia.2012.08.004.
Turner, D., Lewis, M., Ostendorf, B., 2011. Spatial indicators of fire risk in the arid and semi-arid zone of Australia. Ecological Indicators 11, 149-167, doi: https://doi.org/10.1016/j.ecolind.2009.09.001.
Vacek, Z., Rehacek, D., Cukor, J., Vacek, S., Khel, T., Sharma, R.P., Kucera, J., Kral, J., Papaj, V., 2018. Windbreak Efficiency in Agricultural Landscape of the Central Europe: Multiple Approaches to Wind Erosion Control. Environmental Management 62, 942-954, doi: https://doi.org/10.1007/s00267-018-1090-x.
Van Jaarsveld, F., 2008. Characterising and mapping of wind transported sediment associated with opencast gypsum mining. Stellenbosch: Stellenbosch University, http://hdl.handle.net/10019.1/2352
Vermeire, L.T., Wester, D.B., Mitchell, R.B., Fuhlendorf, S.D., 2005. Fire and Grazing Effects on Wind Erosion, Soil Water Content, and Soil Temperature. Journal of Environmental Quality 34, 1559-1565, doi: https://doi.org/10.2134/jeq2005.0006.
Wagenbrenner, N.S., Germino, M.J., Lamb, B.K., Robichaud, P.R., Foltz, R.B., 2013. Wind erosion from a sagebrush steppe burned by wildfire: Measurements of PM10 and total horizontal sediment flux. Aeolian Research 10, 25-36, doi: https://doi.org/10.1016/j.aeolia.2012.10.003.
Webb, N., Herrick, J., Van Zee, J., Hugenholtz, C., Zobeck, T., Okin, G., 2015. Standard Methods for Wind Erosion Research and Model Development: Protocol for the National Wind Erosion Research Network. USDA-ARS Jornada Experimental Range, Las Cruces, New Mexico, https://winderosionnetwork.org/files/NetworkManual.pdf
Webb, N.P., Herrick, J.E., Van Zee, J.W., Courtright, E.M., Hugenholtz, C.H., Zobeck, T.M., Okin, G.S., Barchyn, T.E., Billings, B.J., Boyd, R., Clingan, S.D., Cooper, B.F., Duniway, M.C., Derner, J.D., Fox, F.A., Havstad, K.M., Heilman, P., LaPlante, V., Ludwig, N.A., Metz, L.J., Nearing, M.A., Norfleet, M.L., Pierson, F.B., Sanderson, M.A., Sharratt, B.S., Steiner, J.L., Tatarko, J., Tedela, N.H., Toledo, D., Unnasch, R.S., Van Pelt, R.S., Wagner, L., 2016. The National Wind Erosion Research Network: Building a standardized long-term data resource for aeolian research, modeling and land management. Aeolian Research 22, 23-36, doi: http://dx.doi.org/10.1016/j.aeolia.2016.05.005.
Whicker, J.J., Breshears, D.D., Wasiolek, P.T., Kirchner, T.B., Tavani, R.A., Schoep, D.A., Rodgers, J.C., 2002. Temporal and Spatial Variation of Episodic Wind Erosion in Unburned and Burned Semiarid Shrubland. Journal of Environmental Quality 31, 599-612, doi: https://doi.org/10.2134/jeq2002.5990.
Whicker, J.J., Pinder, J.E., Breshears, D.D., 2006. Increased wind erosion from forest wildfire: Implications for contaminant-related risks. Journal of Environmental Quality 35, 468-478, doi: https://doi.org/10.2134/jeq2005.0112.
Williams, R.J., Bradstock, R.A., Cary, G.J., Enright, N.J., Gill, A.M., Liedloff, A.C., Lucas, C., Whelan, R.J., Andersen, A.N., Bowman, D.M.J.S., Clarke, P.J., Cook, G.D., Hennessy, K.J., York, A., 2009. Interactions between climate change, fire regimes and biodiversity in Australia - a preliminary assessment. Department of Climate Change,

Department of the Environment, Water, Heritage and the Arts, Canberra, http://researchrepository.murdoch.edu.au/id/eprint/14926
Wilson, S., Cooke, R., 1980. Wind erosion, Kirby, M.J, Morgan, R.P.C. (Eds.), Soil erosion. Wiley, Chichester, pp. 217-251,
Zobeck, T., 2002. Field measurement of erosion by wind, Encyclopedia of Soil Science, Marcel Dekker, Inc., New York, pp. 503-507,
Zobeck, T.M., Sterk, G., Funk, R., Rajot, J.L., Stout, J.E., Van Pelt, R.S., 2003. Measurement and data analysis methods for field-scale wind erosion studies and model validation. Earth Surface Processes and Landforms 28, 1163-1188, doi: https://doi.org/10.1002/esp.1033.